

## ORIGINAL ARTICLE

# Characterization of poly(*N,N*-diethylacrylamide) and cloud points in its aqueous solutions

Ryota Watanabe<sup>1</sup>, Kenichi Takaseki<sup>1</sup>, Motoyuki Katsumata<sup>1</sup>, Daiki Matsushita<sup>1</sup>, Daichi Ida<sup>2</sup> and Masashi Osa<sup>1</sup>

The mean-square radius of gyration, second virial coefficient and intrinsic viscosity were determined in methanol at 25.0 °C for two types of poly(*N,N*-diethylacrylamide) (PDEA) samples that were synthesized by radical polymerization in *tert*-butanol and benzene using azobis(isobutyronitrile) as an initiator. Analyses of these results indicated that the primary structure of both PDEA samples was linear. The cloud points of the two PDEA samples were also determined in aqueous solutions. For the two types of PDEA samples, the cloud point decreased as the weight-average molecular weight  $M_w$  of the sample increased, which is in contrast to previously reported results for poly(*N*-isopropylacrylamide) (PNIPA) samples, even though those samples have the same hydrophobic chain-end groups. In addition, the cloud-point curve of each PDEA sample has a critical point, which has not been previously reported for PNIPA. The critical point shifted to the upper right with decreasing  $M_w$ , as predicted by conventional polymer solution thermodynamics. Therefore, the aqueous PDEA solutions exhibited typical phase behavior that is consistent with the lower critical solution temperature type, which is substantially different from that observed for aqueous PNIPA solutions.

*Polymer Journal* (2016) 48, 621–628; doi:10.1038/pj.2015.120; published online 6 January 2016

## INTRODUCTION

Aqueous solutions of some water-soluble polymers exhibit lower critical solution temperature miscibility behaviors, which are caused by the breakdown of hydrogen bonds between the polymers and the surrounding water molecules.<sup>1</sup> Among these water-soluble polymers, poly(*N*-isopropylacrylamide) (PNIPA) has been the most extensively studied from both fundamental and practical points of view, because its aqueous solutions possess cloud points near human body temperature.<sup>2</sup> In addition, the solutions exhibit potential for application to drug-delivery devices and intelligent materials.<sup>3,4</sup>

In recent years, we performed a series of detailed experimental studies on the phase behavior of aqueous PNIPA solutions,<sup>5–9</sup> and found that the observed behavior was not as simple as previously believed. (1) The cloud points in the aqueous solutions of the PNIPA samples, which have hydrophobic isobutyronitrile groups at the chain ends and were synthesized by radical polymerization with azobis(isobutyronitrile) (AIBN) as an initiator in *tert*-butanol and benzene, which are referred to as the PNIPA-T and PNIPA-B samples, respectively, are appreciably higher for the PNIPA-T samples than for the PNIPA-B samples, even though the samples have the same weight-average molecular weight  $M_w$  and stereochemical composition specified by the fraction  $f_r$  of raceme diads.<sup>5</sup> (2) The two types of PNIPA samples have branched structures, and the number of branch points is larger for the PNIPA-B samples than for the PNIPA-T ones.<sup>6</sup> (3) The cloud points in the aqueous solutions of both the PNIPA-T and PNIPA-B samples decreased with decreasing  $M_w$ ,<sup>5</sup> which is in contradiction to the prediction based on conventional polymer

solution thermodynamics<sup>10</sup> and is regarded as arising from effects of their hydrophobic chain-end groups.<sup>7</sup> (4) The cloud points in aqueous solutions of the PNIPA samples synthesized by aqueous redox polymerization, which are referred to as the PNIPA-R samples having hydrophilic sulfonate groups at the chain ends, are definitely higher than those of the PNIPA-T and PNIPA-B samples. In addition, the cloud points of the PNIPA-R samples increase with decreasing  $M_w$ , which is in contrast to the results for the PNIPA-T and PNIPA-B samples.<sup>9</sup> All of these results indicate that the phase behavior of aqueous PNIPA solutions is governed not only by the hydrogen bonds between PNIPA and the surrounding water molecules but also by the end groups and primary structure of the PNIPA chains. In addition, Tong *et al.*<sup>11</sup> observed that the cloud points in aqueous solutions of a given PNIPA sample continue to decrease as the PNIPA concentration  $c$  increased from 0 up to ~70 wt%, and therefore the minimum point of the cloud point curve (that is, the critical point) did not appear. This result indicates that the aqueous PNIPA solutions do not necessarily separate into two liquid phases, (that is, dilute and concentrated ones), when the temperature is increased above their cloud points.

Under these circumstances, further investigations of the aqueous solution behavior of another acrylamide-based polymer, that is, poly(*N,N*-diethylacrylamide) (PDEA), are required, to confirm whether or not the above-mentioned salient features that were observed in the phase behavior of aqueous PNIPA solutions are common to them. Therefore, we proceed to make a study of aqueous PDEA solutions in the same spirit as that in the previous studies<sup>5–9</sup> for PNIPA. Until now,

<sup>1</sup>Department of Chemistry, Aichi University of Education, Kariya, Japan and <sup>2</sup>Department of Polymer Chemistry, Kyoto University, Katsura, Kyoto, Japan  
Correspondence: Dr M Osa, Department of Chemistry, Aichi University of Education, Kariya 448-8542, Japan.  
E-mail: mosa@aeu.ac.jp

Received 25 August 2015; revised 10 November 2015; accepted 10 November 2015; published online 6 January 2016

**Table 1** Values of  $M_w/M_n$  and  $f_r$  and results of LS and viscosity measurements for two types of poly(*N,N*-diethylacrylamide) samples in methanol at 25.0 °C

| Sample  | $M_w/M_n$ | $f_r$             | $M_w$              | $10^4 A_2$ (cm <sup>3</sup> mol g <sup>-2</sup> ) | $10^{-2} \langle S^2 \rangle$ (nm <sup>2</sup> ) | $[\eta]$ (dl g <sup>-1</sup> ) | $k'$ |
|---|-----------|-------------------|--------------------|---|--|--------------------------------|------|
| <i>PDEA-T samples synthesized in tert-butanol</i> |           |                   |                    |   |  |                                |      |
| PDEA-T4   | 1.20      | —                 | $3.85 \times 10^4$ | 5.47  | —  | —                              | —    |
| PDEA-T7   | 1.20      | 0.60 <sub>5</sub> | $6.95 \times 10^4$ | 4.56  | —  | —                              | —    |
| PDEA-T11  | 1.14      | —                 | $1.14 \times 10^5$ | 4.04  | —  | —                              | —    |
| PDEA-T16  | 1.10      | —                 | $1.57 \times 10^5$ | 3.61  | —  | 0.440                          | 0.40 |
| PDEA-T20  | 1.09      | —                 | $2.06 \times 10^5$ | 3.42  | —  | —                              | —    |
| PDEA-T27  | 1.12      | —                 | $2.69 \times 10^5$ | 3.21  | 2.99   | 0.658                          | 0.35 |
| PDEA-T40  | 1.10      | —                 | $3.98 \times 10^5$ | 2.83  | 4.80   | 0.839                          | 0.32 |
| PDEA-T55  | 1.16      | —                 | $5.52 \times 10^5$ | 2.72  | 7.73   | —                              | —    |
| PDEA-T59  | 1.10      | —                 | $5.87 \times 10^5$ | 2.58  | 9.06   | —                              | —    |
| PDEA-T67  | 1.22      | —                 | $6.70 \times 10^5$ | 2.49  | 10.8   | —                              | —    |
| PDEA-T80  | 1.30      | —                 | $7.99 \times 10^5$ | 2.33  | 12.3   | 1.32                           | 0.36 |
| PDEA-T139   | 1.12      | 0.61 <sub>9</sub> | $1.39 \times 10^6$ | 2.14  | 24.0   | 2.18                           | 0.32 |
| <i>PDEA-B samples synthesized in benzene</i>      |           |                   |                    |   |  |                                |      |
| PDEA-B18  | 1.23      | —                 | $1.77 \times 10^5$ | 3.37  | —  | 0.473                          | 0.32 |
| PDEA-B28  | 1.16      | 0.51 <sub>7</sub> | $2.81 \times 10^5$ | 2.94  | 4.12   | 0.729                          | 0.40 |
| PDEA-B39  | 1.21      | —                 | $3.86 \times 10^5$ | 2.85  | 6.35   | —                              | —    |
| PDEA-B51  | 1.12      | —                 | $5.08 \times 10^5$ | 2.71  | 9.30   | 1.12                           | 0.36 |
| PDEA-B63  | 1.15      | —                 | $6.27 \times 10^5$ | 2.43  | 11.3   | —                              | —    |
| PDEA-B85  | 1.24      | —                 | $8.54 \times 10^5$ | 2.20  | 16.2   | —                              | —    |
| PDEA-B115   | 1.22      | —                 | $1.15 \times 10^6$ | 2.11  | 22.8   | 1.64                           | 0.38 |
| PDEA-B122   | 1.23      | 0.51 <sub>9</sub> | $1.22 \times 10^6$ | 2.04  | 24.9   | —                              | —    |
| PDEA-B158   | 1.26      | —                 | $1.58 \times 10^6$ | 1.82  | 38.4   | 2.33                           | 0.41 |

Abbreviations:  $A_2$ , second virial coefficient;  $f_r$ , fraction of raceme diad; PDEA, poly(*N,N*-diethylacrylamide);  $k'$ , Huggins coefficient; LS, light scattering;  $[\eta]$ , intrinsic viscosity;  $M_n$ , number-average molecular weight;  $M_w$ , weight-average molecular weight;  $\langle S^2 \rangle$ , mean-square radius of gyration.

several studies have been performed to study the phase behavior of aqueous PDEA solutions. Lessard *et al.*<sup>12</sup> reported the molecular weight dependence of cloud point curves for PDEA synthesized by aqueous redox polymerization. Freitag *et al.*,<sup>13</sup> Kobayashi *et al.*<sup>14,15</sup> and Katsumoto *et al.*<sup>16</sup> reported the effects of the stereochemical composition on the cloud points of PDEA. Itakura *et al.*<sup>17</sup> studied the aggregation behavior of isotactic PDEA samples in aqueous solutions by using light-scattering (LS) techniques. Maeda *et al.*<sup>18</sup> investigated the changes in the hydration states of PDEA during phase transition by using infrared spectroscopy. However, the effects of the chain-end groups and the primary structure of the PDEA chains on the phase behavior of aqueous PDEA solutions have not yet been studied. Moreover, none of the prior studies have demonstrated the existence of a critical point in the phase diagram of aqueous PDEA solutions. Therefore, in this study, we prepared PDEA samples by radical polymerization with AIBN in *tert*-butanol and benzene, as in the cases of the PNIPA samples. Then, the PDEA samples were characterized to confirm their primary structures by analyzing the mean-square radius of gyration ( $\langle S^2 \rangle$ ) and second virial coefficient  $A_2$ , which were determined from LS measurements, and the intrinsic viscosity  $[\eta]$ , which was determined from viscosity measurements. These experiments were performed in methanol at 25.0 °C. In addition, the values of  $f_r$  of the PDEA samples were determined from <sup>13</sup>C NMR spectra. Then, the cloud points in the aqueous solutions of the two types of PDEA samples were determined, to examine the effects of the hydrophobic chain ends and the primary structure of the PDEA samples on the phase behavior of their aqueous solutions, and also to confirm whether or not their cloud point curves have critical points.

## EXPERIMENTAL PROCEDURE

### Materials

Two types of original PDEA samples were synthesized by radical polymerization in *tert*-butanol and benzene using AIBN as an initiator. In each solvent, *N,N*-diethylacrylamide (Kohjin, Tokyo, Japan), which was purified by distillation under reduced pressure, was polymerized with AIBN under argon at 60 °C for 24 h. The synthesized samples were purified by reprecipitation from acetone solutions into hexane. Then, the resulting polymers were dissolved in pure water and dialyzed seven times against pure water for 24 h using a cellulose tube. The prepared samples were separated into fractions with narrow molecular weight distributions by fractional precipitation using acetone as the solvent and hexane as the precipitant. Each of the test samples so prepared was dissolved in 1,4-dioxane, then filtered through a Teflon membrane with a pore size of 0.45 μm, and finally freeze-dried from the 1,4-dioxane solutions. It is important to note that almost all of the chain ends of the PDEA samples are considered to be the hydrophobic isobutyronitrile groups derived from AIBN.

The codes for all 21 samples used in this study are listed in the first column of Table 1, where the PDEA samples synthesized in *tert*-butanol and benzene are generally referred to as the PDEA-T and PDEA-B samples, respectively. The ratios of the  $M_w$  to the number-average molecular weight  $M_n$  are listed in the second column of Table 1, and these ratios were determined using analytical gel permeation chromatography with two serially connected columns, that is, SB-805HQ and SB-804HQ (Showa Denko KK, Tokyo, Japan), connected to an L-7100 solvent delivery pump (Hitachi, Tokyo, Japan) and a RI-930 refractive index detector (JASCO Corporation, Tokyo, Japan). *N,N*-dimethylformamide containing 10 mM lithium bromide at 50 °C was used as the eluent, and 12 standard polystyrene samples (Tosoh Corporation, Tokyo, Japan,  $M_w = 550 - 5.46 \times 10^6$ ) were used as reference standards.

The methanol solvent used for LS and the viscosity measurements was purified by distillation. The *N,N*-dimethylformamide that was used for analytical gel permeation chromatography was of reagent grade and used without further purification. The deuterated chloroform that was used for <sup>13</sup>C NMR spectroscopy was of reagent grade and used without further purification.

The water that was used for the determinations of the cloud points was highly purified through an Autopure WT101UV water purification system (Yamatō Scientific, Tokyo, Japan), and its resistivity was 18.2 M $\Omega$  cm.

### Light scattering

LS measurements were carried out to determine the  $M_w$  and  $A_2$  for all the 21 PDEA samples and  $\langle S^2 \rangle$  for 15 PDEA samples with  $M_w \geq 2.5 \times 10^5$ , in methanol at 25.0 °C. The measurements were performed using a Wyatt DAWN EOS multi-angle laser LS detector (Wyatt Technology Corporation, Santa Barbara, CA, USA) with incident light of wavelength of 690 nm in micro-batch mode. The multi-angle laser LS detector was calibrated with pure toluene and normalized with an  $\sim 1$  wt% methanol solution containing the poly(ethylene glycol) sample with  $M_w \approx 8 \times 10^3$  (MP Biomedicals, LLC., Solon, OH, USA). The scattered intensity was measured at five different concentrations for each sample. The obtained data were processed using the Berry square-root plot.<sup>19</sup> (Some typical examples of the Berry square-root plots for the PDEA samples in methanol at 25.0 °C are shown in Supplementary Figures S. I. 1 and S. I. 2 in the Supplementary Information.)

The most concentrated solution of each sample was prepared gravimetrically, and continuous stirring at room temperature for 1 or 2 days ensured homogeneity. The sample was optically purified by filtration through a Teflon membrane with a pore size of 0.1  $\mu\text{m}$ . The lower concentration solutions were prepared by successive dilution. The polymer mass concentrations  $c$  of the test solutions were calculated from the weight concentrations of the solutions using the density of the solvent methanol. A literature value of 0.7866 g cm<sup>-3</sup> was used for the density of methanol at 25.0 °C.<sup>20</sup>

The refractive index increment  $\partial n/\partial c$  was measured at a wavelength of 690 nm using an interferometric refractometer OPTILAB DSP (Wyatt Technology Corporation). The refractometer was calibrated with aqueous solutions of anhydrous sodium chloride. The values of  $\partial n/\partial c$  were determined to be 0.175 cm<sup>3</sup> g<sup>-1</sup> for all of the PDEA samples in methanol at 25.0 °C.

### Viscosity

Viscosity measurements were performed for five PDEA-T samples (PDEA-T16, PDEA-T27, PDEA-T40, PDEA-T80 and PDEA-T139) and five PDEA-B samples (PDEA-B18, PDEA-B28, PDEA-B51, PDEA-B115 and PDEA-B158)

in methanol at 25.0 °C using a conventional capillary viscometer of the Ubbelohde type. The flow time was measured to a precision of 0.1 s, keeping the difference between those of the solvent and the solution larger than 20 s. The test solutions were maintained at a constant temperature within  $\pm 0.01$  °C during the measurements.

The most concentrated solution of each sample was prepared according to the same protocol as that used for the LS measurements. The lower concentration solutions were prepared by successive dilution. The polymer mass concentrations  $c$  were calculated from the weight fractions using the density of the solvent methanol. The data obtained for the specific viscosity  $\eta_{sp}$  and the relative viscosity  $\eta_r$  were processed using the Huggins ( $\eta_{sp}/c$  vs  $c$ ) and Fuoss–Meade ( $\ln \eta_r/c$  vs  $c$ ) plots, respectively, to determine  $[\eta]$  and the Huggins coefficient  $k'$ . (Some typical examples of the Huggins and Fuoss–Meade plots for the PDEA samples in methanol at 25.0 °C are shown in Supplementary Figures S. I. 3 and S. I. 4 in the Supplementary Information.)

### <sup>13</sup>C NMR

The <sup>13</sup>C NMR spectra of two PDEA-T samples (PDEA-T7 and PDEA-T139) and two PDEA-B samples (PDEA-B28 and PDEA-B122) were recorded in deuterated chloroform at 50 °C using a concentration of  $\sim 2$  wt% on a spectrometer JEOL JNM ECA-600 (JEOL, Tokyo, Japan) at 150.9 MHz using a radiofrequency pulse angle of 90 ° and a pulse repetition time of 10 s. A total of 22 000 spectra were accumulated for each sample. Tetramethylsilane was added to each sample as an internal standard.

### Transmittance of light

The intensity of the light passing through the aqueous solutions of six PDEA-T samples (PDEA-T7, PDEA-T11, PDEA-T27, PDEA-T40, PDEA-T80 and PDEA-T139) and four PDEA-B samples (PDEA-B18, PDEA-B28, PDEA-B85 and PDEA-B122) at various weight fractions  $w$  ranging from 0.5 to 25 wt% was measured using a home-made apparatus, which was constructed previously,<sup>5,21</sup> with an incident light of wavelength of 650 nm that was emitted from a laser diode module. A given test solution that was contained in a cylindrical cell with a diameter of 10 mm was immersed in a water bath and continuously stirred. To determine the cloud point of each solution, the temperature of the solution was increased at a rate of  $\sim 1.5$  °C h<sup>-1</sup>. During the continuous temperature increase from  $\sim 26$  °C to  $\sim 34$  °C, the intensity of the light passing through the test solution was monitored by a photodiode. The output of the photodiode, along with the solution temperature which was measured simultaneously, was recorded on a personal computer. Then, the relative transmittance, which is defined as the ratio of the intensity of light passing through the test solution at a given temperature to the intensity at a lower temperature (for which the test solution is transparent), was determined as a function of temperature.

The most concentrated solution of each sample was gravimetrically prepared and was continuously stirred for 2 days at room temperature to ensure homogeneity. The lower concentration solutions were obtained by successive dilution.

## RESULTS AND DISCUSSION

### Characterization

**Stereochemical compositions.** Figure 1 shows the <sup>13</sup>C NMR spectra for the PDEA-T7, PDEA-T139, PDEA-B28 and PDEA-B122 samples from a chemical shift  $\delta$  of 173.3 to 174.5 p.p.m., and the signals from the carbonyl carbon in the side group were observed. According to Kobayashi *et al.*,<sup>15</sup> the signals located at 173.4–173.7 p.p.m., 173.7–174.0 p.p.m. and 174.0–174.3 p.p.m. were owing to the isotactic (*mm*), heterotactic (*mr*), and syndiotactic (*rr*) triads, respectively, although these signals partially overlapped each other. To separate the signals into the contributions from the three types of triads (*mm*, *mr* and *rr*), we assume that the spectra at  $\delta = 173.3$ –174.5 p.p.m. can be represented by a linear combination of three Lorentzians and then determine the coefficient (or weight) as well as the half-width at half-maximum of each Lorentzian using numerical deconvolution under the following constraints: the maximum points of the first, second and

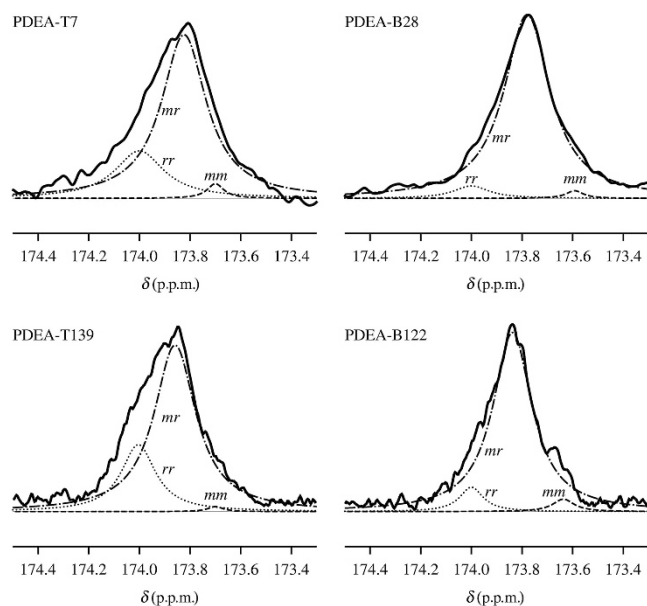


**Figure 1** <sup>13</sup>C NMR spectra of the carbonyl carbon in the side group for the PDEA-T7, PDEA-T139, PDEA-B28 and PDEA-B122 samples. The dashed, dot-dashed and dotted curves represent the Lorentzian components for the *mm*, *mr* and *rr* triads of each sample, respectively. PDEA, poly(*N,N*-diethylacrylamide); PDEA-B, PDEA samples synthesized in benzene; PDEA-T, PDEA samples synthesized in *tert*-butanol.

third Lorentzians are located at  $173.4 \text{ p.p.m.} \leq \delta \leq 173.7 \text{ p.p.m.}$ ,  $173.7 \text{ p.p.m.} \leq \delta \leq 174.0 \text{ p.p.m.}$  and  $174.0 \text{ p.p.m.} \leq \delta \leq 174.3 \text{ p.p.m.}$ , respectively. On the basis of the determined weight of the three Lorentzians, we estimated the fractions of the triads, which are referred to as  $f_{mm}$ ,  $f_{mr}$  and  $f_{rr}$ , for the four samples, as follows:  $f_{mm}=0.02_5$ ,  $f_{mr}=0.74_1$  and  $f_{rr}=0.23_4$  for the sample PDEA-T7;  $f_{mm}=0.00_8$ ,  $f_{mr}=0.74_6$  and  $f_{rr}=0.24_6$  for the sample PDEA-T139;  $f_{mm}=0.01_5$ ,  $f_{mr}=0.93_7$  and  $f_{rr}=0.04_8$  for the sample PDEA-B28; and  $f_{mm}=0.03_4$ ,  $f_{mr}=0.89_4$  and  $f_{rr}=0.07_2$  for the sample PDEA-B122. In Figure 1, the dashed, dot-dashed and dotted curves represent the Lorentzian components for the *mm*, *mr* and *rr* triads, respectively. [The  $^{13}\text{C}$  NMR spectra including the superimposed values ( $mm+mr+rr$ ) and the Lorentzian components for the three types of triads for these PDEA samples are shown in Supplementary Figure S. I. 5 in the Supplementary Information.] The values of  $f_r$  calculated from the following equation,

$$f_r = f_{rr} + \frac{f_{mr}}{2}$$

are provided in the third column of Table 1. The  $f_r$  values of the PDEA-T and PDEA-B samples were  $\sim 0.61$  and  $\sim 0.52$ , respectively, indicating that the former samples are more syndiotactic than the latter ones.

*Mean-square radius of gyration and second virial coefficient in methanol at 25.0 °C.* The values of  $M_w$  and  $A_2$  determined from LS measurements in methanol at 25.0 °C for all the 21 samples are listed in the fourth and fifth columns, respectively, of Table 1. The sixth column of Table 1 provides the values of  $\langle S^2 \rangle$  for the seven PDEA-T samples, that is, PDEA-T27 through PDEA-T139, and the eight PDEA-B samples, that is, PDEA-B28 through PDEA-B158, that were determined simultaneously from the LS measurements in methanol at 25.0 °C. It is important to note that the values of  $\langle S^2 \rangle$  for the samples with  $M_w \lesssim 2.5 \times 10^5$  have been excluded because the slopes of the Berry square-root plots against the square of the magnitude of the scattering vector for these samples are not sufficiently large to allow for accurate evaluation of  $\langle S^2 \rangle$ . The values of  $A_2$  are on the order of  $10^{-4} \text{ cm}^3 \text{ mol g}^{-2}$ , indicating that methanol at 25.0 °C is a good solvent for PDEA.

Figure 2 shows the double-logarithmic plots of  $\langle S^2 \rangle$  (in  $\text{nm}^2$ ) against  $M_w$  for PDEA in methanol at 25.0 °C. The unfilled circles and

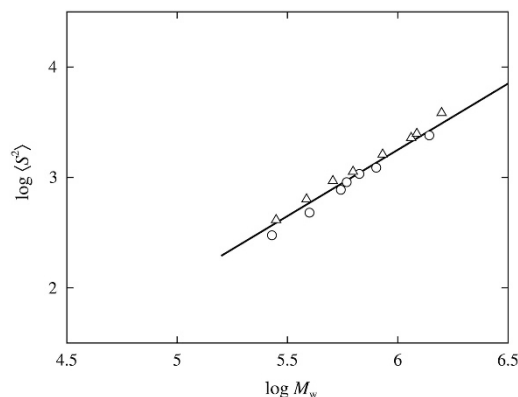


**Figure 2** Double-logarithmic plots of  $\langle S^2 \rangle$  (in  $\text{nm}^2$ ) against  $M_w$  for PDEA in methanol at 25.0 °C: (○) PDEA-T samples; (△) PDEA-B samples. The solid straight line has a slope of 1.2.  $M_w$ , weight-average molecular weight; PDEA, poly(*N,N*-diethylacrylamide); PDEA-B, PDEA samples synthesized in benzene; PDEA-T, PDEA samples synthesized in *tert*-butanol.

triangles represent the values for the PDEA-T and PDEA-B samples, respectively. On the basis of the results in Figure 2, the values of  $\langle S^2 \rangle$  for the two types of PDEA samples are in good agreement with each other. This agreement implies that the difference in the stereochemical compositions between the two types of PDEA samples, which was discussed in the previous subsection, does not appreciably affect the average chain dimension of PDEA in methanol at 25.0 °C. In addition, over the entire  $M_w$  range, all of the data points are in a straight line with a slope of 1.2, which is represented by the solid line in Figure 2. The value 1.2 of the slope is consistent with that for linear<sup>22,23</sup> and star<sup>24</sup> flexible polymers with very large  $M_w$  in good solvents. Therefore, these results indicate that the two types of PDEA behave as flexible polymers in methanol at 25.0 °C, and no difference in the degree of branching was observed between the two types of PDEA samples, in contrast to the previous case<sup>6</sup> of PNIPA. We note that, in the case of PNIPA previously studied,<sup>6</sup> the PNIPA samples synthesized by radical polymerization have branched structures, and the number of branch points is larger in the PNIPA-B samples (synthesized in benzene) than that in the PNIPA-T samples (synthesized in *tert*-butanol). Therefore, the former PNIPA samples have smaller values of  $\langle S^2 \rangle$  than the latter PNIPA samples when compared at the same  $M_w$  (see Figure 1 in Kawaguchi *et al.*<sup>6</sup>).

Figure 3 shows the double-logarithmic plots of  $A_2$  (in  $\text{cm}^3 \text{ mol g}^{-2}$ ) against  $M_w$  for PDEA in methanol at 25.0 °C. The symbols have the same meaning as those in Figure 2. The values of  $A_2$  for the two types of PDEA samples are in good agreement with each other, similar to the results for the  $\langle S^2 \rangle$  values. The quantity of  $A_2$  is proportional to the effective volume excluded by the polymer chain owing to the presence of another, and therefore the agreement between the  $A_2$  values for the two types of PDEA samples indicates that the effective volume of a given PDEA-T sample is almost the same as that of a given PDEA-B sample with the same  $M_w$ . In addition, the data points are in a straight line with a slope of  $-0.2$ , which is represented by the solid line in the figure, except for the range of small  $M_w$  ( $\lesssim 10^5$ ) where the effects of the chain ends on  $A_2$  becomes appreciable.<sup>23</sup> The value  $-0.2$  of the slope is consistent with that for linear<sup>22,23</sup> and star<sup>24</sup> flexible polymers with very large  $M_w$  in good solvents, which is similar to the results for  $\langle S^2 \rangle$ . In addition, the values of the interpenetration function  $\Psi$ , which is defined as  $\Psi = A_2 M_w^2 / 4\pi^{3/2} N_A \langle S^2 \rangle^{3/2}$  with  $N_A$  the Avogadro constant, estimated for the two types of PDEA samples using the values of  $M_w$ ,  $\langle S^2 \rangle$  and  $A_2$  given in Table 1, are consistent with those for linear flexible polymers<sup>22,23</sup> and smaller than those for star flexible polymers.<sup>24</sup> Therefore, all of these results indicate that both the types of PDEA are linear flexible polymers.

*Intrinsic viscosity in methanol at 25.0 °C.* The values of  $[\eta]$  and  $k'$  determined from viscosity measurements in methanol at 25.0 °C are listed in the seventh and eighth columns, respectively, of Table 1. Figure 4 shows the double-logarithmic plots of  $[\eta]$  (in  $\text{dl g}^{-1}$ ) against  $M_w$  for PDEA in methanol at 25.0 °C. The symbols have the same meaning as those in Figures 2 and 3. Similar to that observed for  $\langle S^2 \rangle$  and  $A_2$  shown in Figures 2 and 3, the data points for the two types of PDEA samples agree well with each other and form a straight line with a slope of 0.7, which is represented by the solid line in Figure 4, over the entire range of  $M_w$ . The value 0.7 of the slope is consistent with that for linear<sup>25</sup> and star<sup>24</sup> flexible polymers with very large  $M_w$  in good solvents. In addition, the values of the Flory-Fox factor  $\Phi$ , which is defined as  $\Phi = M_w [\eta] / (6 \langle S^2 \rangle)^{3/2}$ , estimated for the two types of PDEA samples using the values of  $M_w$ ,  $\langle S^2 \rangle$ , and  $[\eta]$  given in Table 1 are consistent with those for linear flexible polymers in good solvents.<sup>22</sup> Therefore, these results also confirm that the two types



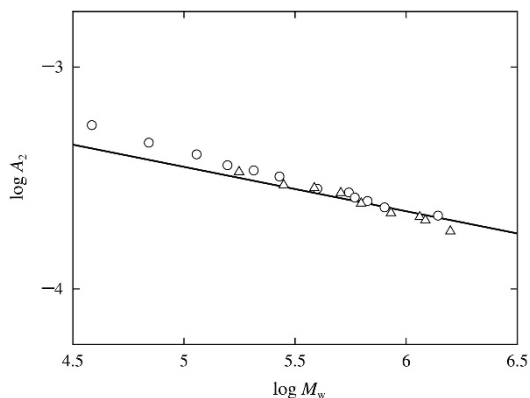


**Figure 3** Double-logarithmic plots of  $A_2$  (in  $\text{cm}^3 \text{mol g}^{-2}$ ) against  $M_w$  for PDEA in methanol at 25.0 °C: (○) PDEA-T samples; (△) PDEA-B samples. The solid straight line has a slope of  $-0.2$ .  $A_2$ , second virial coefficient;  $M_w$ , weight-average molecular weight; PDEA, poly(*N,N*-diethylacrylamide); PDEA-B, PDEA samples synthesized in benzene; PDEA-T, PDEA samples synthesized in *tert*-butanol; ( $S^2$ ), mean-square radius of gyration.

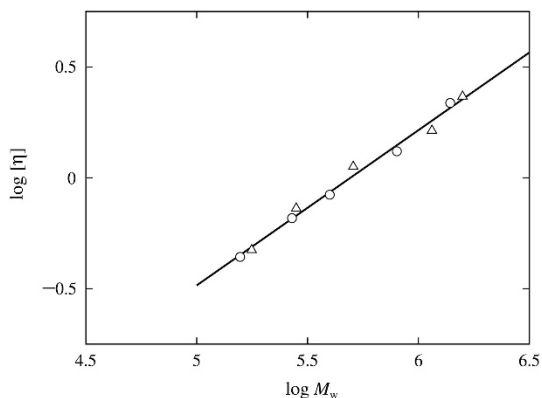


**Figure 4** Double-logarithmic plots of  $[\eta]$  (in  $\text{dl g}^{-1}$ ) against  $M_w$  for PDEA in methanol at 25.0 °C: (○) PDEA-T samples; (△) PDEA-B samples. The solid straight line has a slope of  $0.7$ .  $M_w$ , weight-average molecular weight;  $[\eta]$ , intrinsic viscosity; PDEA, poly(*N,N*-diethylacrylamide); PDEA-B, PDEA samples synthesized in benzene; PDEA-T, PDEA samples synthesized in *tert*-butanol.

of PDEA are linear flexible polymers. It is important to note that, in the previous case for PNIPA,<sup>6</sup> the values of  $[\eta]$  for the PNIPA-B samples are smaller than those for the PNIPA-T samples at the same  $M_w$  because the degree of branching is larger for the former PNIPA samples than for the latter PNIPA ones (see Figure 3 in Kawaguchi *et al.*<sup>6</sup>).

#### Cloud point in aqueous solutions

Figure 5 shows the plots of the (relative) transmittance against temperature for aqueous solutions of six PDEA-T samples, that is, PDEA-T7, PDEA-T11, PDEA-T27, PDEA-T40, PDEA-T80 and PDEA-T139, at a weight fraction  $w=2.72, 3.01, 2.89, 3.02, 3.03$  and  $3.03\%$ , respectively. It is important to note that the shape of the transmittance curve for each solution is nearly independent of the rate of temperature increase when it is slower than  $1.5\text{ °C h}^{-1}$ . The transmittance curve shifts toward the left (low-temperature side) with increasing  $M_w$ , which is in contrast to the behavior of the aqueous solutions of the PNIPA-T samples previously studied,<sup>5</sup> despite both samples being synthesized in the same solvent (*tert*-butanol) and

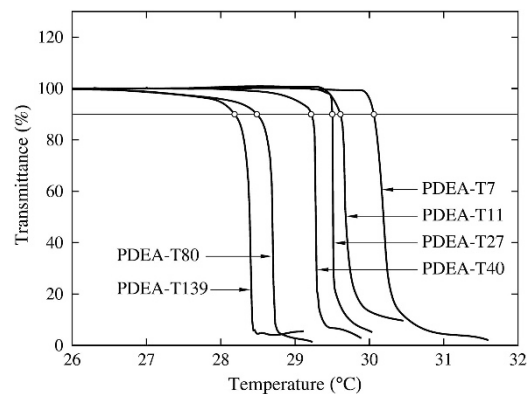


**Figure 5** Temperature dependence of the transmittance of the light passing through aqueous solutions of the PDEA-T7, PDEA-T11, PDEA-T27, PDEA-T40, PDEA-T80 and PDEA-T139 samples at  $w=2.72, 3.01, 2.89, 3.02, 3.03$  and  $3.03\%$ , respectively. The horizontal line indicates the threshold value (90%), and the unfilled circle on each curve indicates the cloud point. PDEA, poly(*N,N*-diethylacrylamide); PDEA-T, PDEA samples synthesized in *tert*-butanol.

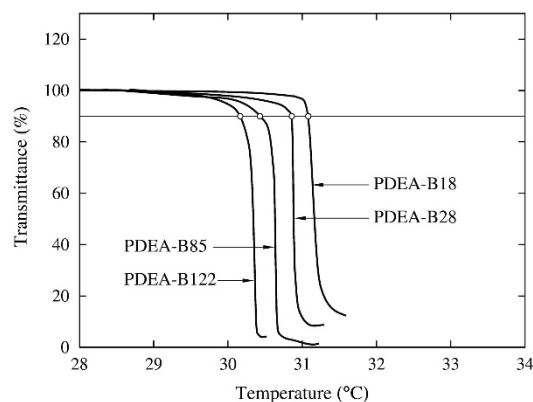


**Figure 6** Temperature dependence of the transmittance of the light passing through aqueous solutions of the PDEA-B18, PDEA-B28, PDEA-B85 and PDEA-B122 samples, at  $w=3.14, 3.00, 3.02$  and  $2.99\%$ , respectively. The horizontal line and the unfilled circles have the same meaning as those in Figure 5. PDEA, poly(*N,N*-diethylacrylamide); PDEA-B, PDEA samples synthesized in benzene.

bearing the same hydrophobic (isobutyronitrile) chain-end groups. Figure 6 shows the plots of the (relative) transmittance against temperature for aqueous solutions of four PDEA-B samples, that is, PDEA-B18, PDEA-B28, PDEA-B85 and PDEA-B122, at  $w=3.14, 3.00, 3.02$  and  $2.99\%$ , respectively. Similar to that observed for the PDEA-T samples, the transmittance curve for the PDEA-B samples shifted toward the left (low-temperature side) with increasing  $M_w$ . In addition, the  $M_w$  dependence is in contrast to that of the aqueous solutions of the PNIPA-B samples previously studied,<sup>5</sup> even though both samples were synthesized in benzene and bear the same hydrophobic isobutyronitrile groups at their chain ends.

In principle, the cloud point in a given test solution is the temperature at which the solution just begins to become turbid. However, this temperature is difficult to determine unambiguously because the transmittance for each solution starts to decrease gently from 100%, as shown in Figures 5 and 6. Therefore, following the previous studies for PNIPA,<sup>5,9</sup> the cloud point in each solution was determined to be the temperature at which the transmittance becomes

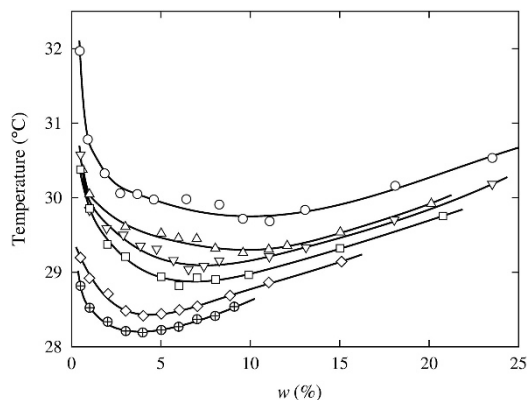


**Figure 7** Cloud-point curves in aqueous solutions of the PDEA-T samples: (○) PDEA-T7, (△) PDEA-T11, (▽) PDEA-T27, (□) PDEA-T40, (◇) PDEA-T80 and (⊕) PDEA-T139. The solid curves smoothly connect the respective data points. PDEA, poly(*N,N*-diethylacrylamide); PDEA-T, PDEA samples synthesized in *tert*-butanol.

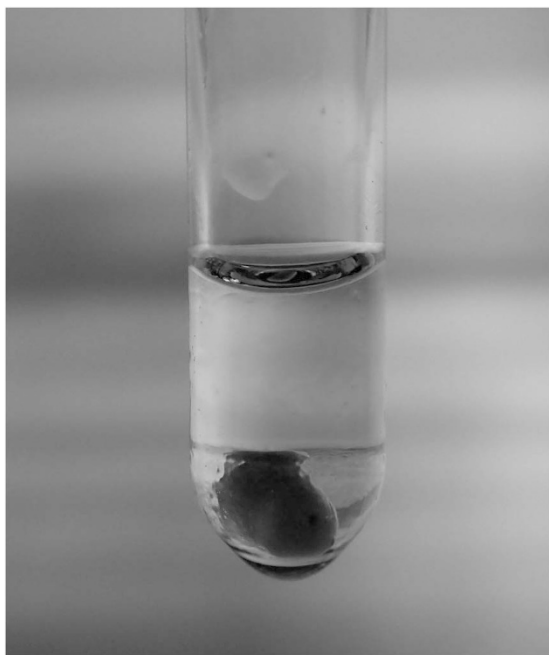


**Figure 8** Photograph of an aqueous solution of the PDEA-T11 sample at ~10% and at ~34 °C. The phase separation into two transparent liquid phases is visible. PDEA, poly(*N,N*-diethylacrylamide); PDEA-T, PDEA samples synthesized in *tert*-butanol. A full color version of this figure is available at *Polymer Journal* online.

a threshold value of 90%. The cloud points for the aqueous solutions of the six PDEA-T samples (PDEA-T7, PDEA-T11, PDEA-T27, PDEA-T40, PDEA-T80 and PDEA-T139) and the four PDEA-B samples (PDEA-B18, PDEA-B28, PDEA-B85 and PDEA-B122) at other  $w$  values were also determined in the same manner as that mentioned above.

Figure 7 shows the cloud-point curves in aqueous solutions of the PDEA-T samples, that is, PDEA-T7 (○), PDEA-T11 (△), PDEA-T27 (▽), PDEA-T40 (□), PDEA-T80 (◇) and PDEA-T139 (⊕). The solid curves connect smoothly the cloud points for the respective PDEA-T samples. As expected from the result shown in Figure 5, the cloud point at a given  $w$  decreased as  $M_w$  increased, which is consistent with

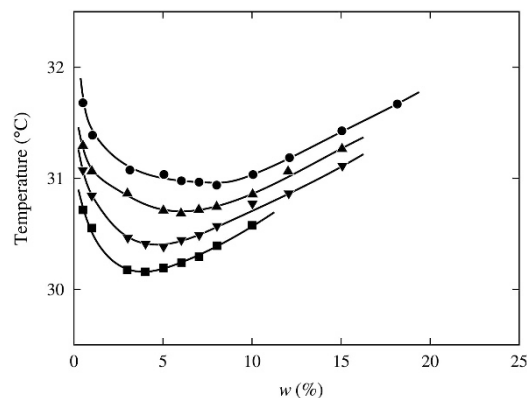


**Figure 9** Cloud-point curves in aqueous solutions of the PDEA-B samples: (●) PDEA-B18, (▲) PDEA-B28, (▼) PDEA-B85 and (■) PDEA-B122. The solid curves smoothly connect the respective data points. PDEA, poly(*N,N*-diethylacrylamide); PDEA-B, PDEA samples synthesized in benzene.

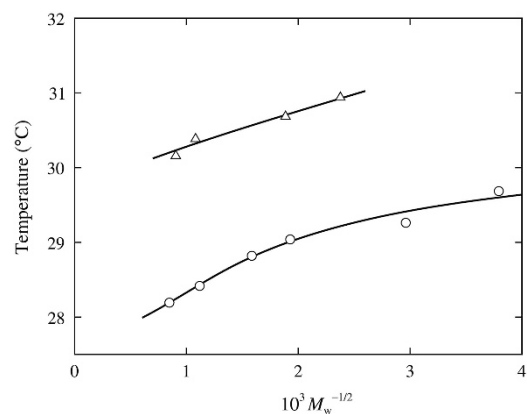


**Figure 10** Plots of the critical point temperature against  $M_w^{-1/2}$  for aqueous PDEA solutions: (○) PDEA-T samples; (△) PDEA-B samples. The solid curve smoothly connects the data points for each type of PDEA.  $M_w$ , weight-average molecular weight; PDEA, poly(*N,N*-diethylacrylamide); PDEA-B, PDEA samples synthesized in benzene; PDEA-T, PDEA samples synthesized in *tert*-butanol.

the conclusion derived from polymer solution thermodynamics<sup>10</sup> and in contrast to the previous results<sup>5</sup> obtained for the PNIPA-T samples. It is important to note that the increase in the cloud point with increasing  $M_w$ , which was observed for the PNIPA-T samples, may be regarded as arising from the effects of their hydrophobic (isobutyronitrile) chain-end groups.<sup>5,7</sup> However, for the PDEA-T samples, the same hydrophobic chain-end groups appear to have little influence on the behavior of the cloud point of the PDEA-T samples. The reason for the difference in the chain-end effects on the cloud point between PNIPA and PDEA remains unclear and will be studied in the future. It is more important to note that the cloud-point curve for each PDEA-T sample has a critical point, and these critical points have not been previously observed for aqueous PNIPA solutions.<sup>11</sup> In particular, the cloud point for each PDEA-T sample decreased as  $w$  increased to the critical point and then increased inversely at the critical point. The existence of the critical points on the cloud-point curves indicates that the aqueous solutions of the PDEA-T samples exhibit liquid-liquid phase separation into two liquid phases, that is, dilute and concentrated phases, as the temperature is increased above the cloud points. In fact, the phase separation was observed for all of the aqueous solutions of the studied PDEA-T samples. For example, Figure 8

shows a photograph of the aqueous solution of the PDEA-T11 sample at  $\sim 10\%$  and at  $\sim 34^\circ\text{C}$ , and this image shows the phase separation, resulting in two transparent liquid phases. As shown in Figure 7, the critical point associated with each cloud-point curve tends to move to the upper right as  $M_w$  decreased. This behavior can be understood on the basis of conventional polymer solution thermodynamics.<sup>10</sup> Therefore, the aqueous solutions of the PDEA-T samples exhibit a typical (and normal) lower critical solution temperature type phase diagram, which is substantially different from that observed for the PNIPA-T samples.

Figure 9 shows the cloud-point curves for the aqueous solutions of the PDEA-B samples, that is, PDEA-B18 (●), PDEA-B28 (▲), PDEA-B85 (▼) and PDEA-B122 (■). The solid curves connect smoothly the cloud points for the respective PDEA-B samples. Similar to the results for the PDEA-T samples, the cloud points for the PDEA-B samples at a given  $w$  decreased with increasing  $M_w$ , and each of the cloud-point curves for the PDEA-B samples has a critical point. The critical point appears to move to the upper right as  $M_w$  decreased. On the basis of these observations, the aqueous solutions of the PDEA-B samples also exhibit typical (and normal) lower critical solution temperature type phase behavior as well as those of the PDEA-T samples.

For PNIPA, the cloud point in the aqueous solution of the PNIPA-B sample was lower than that of the PNIPA-T sample at the same  $M_w$ , even though the two types of PNIPA samples have the same hydrophobic chain-end groups and nearly the same value of  $f_r$ .<sup>5</sup> The difference in the cloud points between the PNIPA-T and PNIPA-B samples may be caused by the difference in the degree of branching between them (that is, the number of branch points is smaller for the former than for the latter).<sup>6</sup> An increase in the number of branch points occurs owing to an increase in the number of the hydrophobic chain-end groups, which may be the reason for the difference in the cloud points between the PNIPA-T and PNIPA-B samples. Under these circumstances, it is interesting to compare the cloud points of the two types of PDEA samples used in the current study. Figure 10 shows the plots of the critical point temperature against  $M_w^{-1/2}$  for the aqueous solutions of the six PDEA-T samples (PDEA-T7, PDEA-T11, PDEA-T27, PDEA-T40, PDEA-T80 and PDEA-T139) and the four PDEA-B samples (PDEA-B18, PDEA-B28, PDEA-B85 and PDEA-B122). The unfilled circles and triangles represent the values for the PDEA-T and PDEA-B samples, respectively. The critical point temperature for each sample is defined as the minimum of its cloud-point curve. However, for convenience in this study, the critical point temperature was determined to be the lowest value of the cloud points measured for each sample. The solid curve connects smoothly the data points for each type of PDEA. In the whole range of  $M_w$  examined, the critical point temperature is higher for the PDEA-B samples than for the PDEA-T ones when compared at the same  $M_w$ , indicating that the cloud point for the PDEA-B samples is typically higher than that for the PDEA-T samples. In the previous subsection, we confirmed that the primary structure of both the PDEA-T and PDEA-B samples is linear, and the two types of PDEA samples have no branch points. However, the stereochemical composition of each type of sample varies, and the PDEA-T samples are more syndiotactic than the PDEA-B samples. According to Kobayashi *et al.*<sup>15</sup> and Katsumoto *et al.*,<sup>16</sup> the cloud point in aqueous PDEA solutions decreased as the syndiotacticity (or  $f_r$ ) of the PDEA samples increased. Therefore, the difference in the cloud point between the PDEA-T and PDEA-B samples, both having a linear primary structure and the same hydrophobic chain-end groups, is caused by the difference in the stereochemical composition between the two types of PDEA samples.

## CONCLUSION

We have determined  $\langle S^2 \rangle$ ,  $A_2$  and  $[\eta]$  in methanol at  $25.0^\circ\text{C}$  for two types of PDEA samples synthesized by radical polymerization in *tert*-butanol and benzene by the use of AIBN as an initiator, and these samples are referred to as PDEA-T and PDEA-B samples, respectively. All of the  $\langle S^2 \rangle$ ,  $A_2$  and  $[\eta]$  values for the two types of PDEA samples agree well with each other in the studied  $M_w$  range. In addition, the slopes of the double-logarithmic plots of these quantities against  $M_w$  as well as the  $\Psi$  and  $\Phi$  values are consistent with those of linear flexible polymers with large  $M_w$  in good solvents. On the basis of these results, the primary structure of both the PDEA-T and PDEA-B samples is linear. In addition,  $^{13}\text{C}$  NMR spectroscopy was used to determine the  $f_r$  values of the two types of PDEA samples, and the PDEA-T samples were more syndiotactic than the PDEA-B samples.

For the aqueous solutions of the PDEA-T and PDEA-B samples, the cloud-point curves have been determined for a weight fraction  $w$  of 0.5% up to 25%. The cloud point at a given  $w$  decreased with increasing  $M_w$  for both types of PDEA samples, and this  $M_w$  dependence is in contrast to the previous results<sup>5</sup> for PNIPA samples synthesized in *tert*-butanol and benzene with AIBN as an initiator. In addition, the cloud-point curve for each PDEA sample has a critical point, and the aqueous solutions of the PDEA samples exhibit a phase separation into two transparent liquid phases, which has not been previously observed for aqueous PNIPA solutions. The critical point for the PDEA-T and PDEA-B samples moved to the upper right with decreasing  $M_w$ , as predicted from conventional polymer solution thermodynamics.<sup>10</sup> Therefore, the aqueous solutions of the PDEA-T and PDEA-B samples exhibit typical (and normal) lower critical solution temperature type phase diagram which is substantially different from that observed for aqueous PNIPA solutions. Furthermore, the cloud point is typically higher for the PDEA-B samples than for the PDEA-T samples, even though both samples have the same hydrophobic chain-end groups and no branch points. The difference in the cloud point between the two types of PDEA samples may arise from the differences in their stereochemical composition.

## CONFLICT OF INTEREST

The authors declare no conflict of interest.

- 1 Koningsveld, R., Stockmayer, W. H. & Nies, E. *Polymer Phase Diagrams* (Oxford Univ. Press, New York, NY, USA, 2001).
- 2 Schild, H. G. Poly(*N*-isopropylacrylamide): experiment, theory, and application. *Prog. Polym. Sci.* **17**, 163–249 (1992).
- 3 Kikuchi, A. & Okano, T. Pulsatile drug release control using hydrogels. *Adv. Drug Deliv. Rev.* **54**, 53–77 (2002).
- 4 Gil, E. S. & Hudson, S. M. Stimuli-responsive polymers and their bioconjugates. *Prog. Polym. Sci.* **29**, 1173–1222 (2004).
- 5 Kawaguchi, T., Kojima, Y., Osa, M. & Yoshizaki, T. Cloud points in aqueous poly(*N*-isopropylacrylamide) solutions. *Polym. J.* **40**, 455–459 (2008).
- 6 Kawaguchi, T., Kojima, Y., Osa, M. & Yoshizaki, T. Primary structure of poly(*N*-isopropylacrylamide) synthesized by radical polymerization. Effects of polymerization solvents. *Polym. J.* **40**, 528–533 (2008).
- 7 Kobayashi, K., Yamada, S., Nagaoka, K., Kawaguchi, T., Osa, M. & Yoshizaki, T. Characterization of linear poly(*N*-isopropylacrylamide) and cloud points in its aqueous solutions. *Polym. J.* **41**, 416–424 (2009).
- 8 Kawaguchi, T., Kobayashi, K., Osa, M. & Yoshizaki, T. Is a 'cloud-point curve' in aqueous poly(*N*-isopropylacrylamide) solution binodal? *J. Phys. Chem. B* **113**, 5440–5447 (2009).
- 9 Ise, T., Nagaoka, K., Osa, M. & Yoshizaki, T. Cloud points in aqueous solutions of poly(*N*-isopropylacrylamide) synthesized by aqueous redox polymerization. *Polym. J.* **43**, 164–170 (2011).
- 10 Flory, P. J. *Principles of Polymer Chemistry* (Cornell Univ. Press, Ithaca, NY, USA, 1953).

- 11 Tong, Z., Zeng, F. & Zheng, X. Inverse molecular weight dependence of cloud points for aqueous poly(*N*-isopropylacrylamide) solutions. *Macromolecules* **32**, 4488–4490 (1999).
- 12 Lessard, D. G., Ousalem, M. & Zhu, X. X. Effect of the molecular weight on the lower critical solution temperature of poly(*N,N*-diethylacrylamide) in aqueous solutions. *Can. J. Chem.* **79**, 1870–1874 (2001).
- 13 Freitag, R., Baltes, T. & Eggert, M. A comparison of thermoreactive water-soluble poly-*N,N*-diethylacrylamide prepared by anionic and by group transfer polymerization. *J. Polym. Sci. A Polym. Chem.* **32**, 3019–3030 (1994).
- 14 Kobayashi, M., Okuyama, S., Ishizone, T. & Nakahama, S. Stereospecific anionic polymerization of *N,N*-diethylacrylamides. *Macromolecules* **32**, 6466–6477 (1999).
- 15 Kobayashi, M., Ishizone, T. & Nakahama, S. Synthesis of highly isotactic poly(*N,N*-diethylacrylamide) by anionic polymerization with Grignard reagents and diethylzinc. *J. Polym. Sci. A Polym. Chem.* **38**, 4677–4685 (2000).
- 16 Katsumoto, Y., Etoh, Y. & Shimoda, N. Phase diagrams of stereocontrolled poly(*N,N*-diethylacrylamide) in water. *Macromolecules* **43**, 3120–3121 (2010).
- 17 Itakura, M., Inomata, K. & Nose, T. Aggregation behavior of poly(*N,N*-diethylacrylamide) in aqueous solution. *Polymer* **41**, 8681–8687 (2000).
- 18 Maeda, Y., Nakamura, T. & Ikeda, I. Change in solvation of poly(*N,N*-diethylacrylamide) during phase transition in aqueous solutions as observed by IR spectroscopy. *Macromolecules* **35**, 10172–10177 (2002).
- 19 Berry, G. C. Thermodynamic and conformational properties of polystyrene. I. Light-scattering studies on dilute solutions of linear polystyrenes. *J. Chem. Phys.* **44**, 4550–4564 (1966).
- 20 Johnson, B. L. & Smith, J. in *Light Scattering from Polymer Solutions* (ed. Huglin, M. B.) Ch. 2 (Academic, London, UK, 1972).
- 21 Osa, M., Shiraki, H., Morinaga, U. & Yoshizaki, T. Effects of surfactants on cloud points in aqueous poly(*N*-isopropylacrylamide) solutions. *Polym. J.* **45**, 681–684 (2013).
- 22 Yamakawa, H. *Modern Theory of Polymer Solutions* (Harper & Row, New York, NY, USA, 1971).
- 23 Yamakawa, H. *Helical Wormlike Chains in Polymer Solutions* (Springer, Berlin, Germany, 1997).
- 24 Nakamura, Y. Dilute solution properties of star and comb polymers. *Kobunshi Ronbunshu* **57**, 530–541 (2000).
- 25 Abe, F., Einaga, Y. & Yamakawa, H. Excluded-volume effects on the intrinsic viscosity of oligomers and polymers of styrene and isobutylene. *Macromolecules* **26**, 1891–1897 (1993).

Supplementary Information accompanies the paper on Polymer Journal website (<http://www.nature.com/pj>)